J. Biochem. **133**, 553–562 (2003)
DOI: 10.1093/jb/mvg071

Xylose Reductase from the Basidiomycete Fungus *Cryptococcus flavus*: Purification, Steady-State Kinetic Characterization, and Detailed Analysis of the Substrate Binding Pocket Using Structure–Activity Relationships

Peter Mayr[1,2], Barbara Petschacher[1] and Bernd Nidetzky[1,*]

[1]Institute of Biotechnology, Graz University of Technology, Petersgasse 12/I, A-8010 Graz, Austria; and [2]Institute of Food Technology, University of Agricultural Sciences Vienna, Muthgasse 18, A-1190 Vienna, Austria

Received November 22, 2002; accepted February 7, 2003

Xylose reductase has been purified to apparent homogeneity from cell extracts of the fungus *Cryptococcus flavus* grown on D-xylose as carbon source. The enzyme, the first of its kind from the phylum *Basidiomycota*, is a functional dimer composed of identical subunits of 35.3 kDa mass and requires NADP(H) for activity. Steady-state kinetic parameters for the reaction, D-xylose + NADPH + H^+↔ xylitol + $NADP^+$, have been obtained at pH 7.0 and 25°C. The catalytic efficiency for reduction of D-xylose is 150 times that for oxidation of xylitol. This and the 3-fold tighter binding of NADPH than $NADP^+$ indicate that the enzyme is primed for unidirectional metabolic function in microbial physiology. Kinetic analysis of enzymic reduction of aldehyde substrates differing in hydrophobic and hydrogen bonding capabilities with binary enzyme-NADPH complex has been used to characterize the substrate-binding pocket of xylose reductase. Total transition state stabilization energy derived from bonding with non-reacting sugar hydroxyls is ≈15 kJ/mol, with a major contribution of 5–8 kJ/mol made by interactions with the C-2(*R*) hydroxy group. The aldehyde binding site is ≈1.2 times more hydrophobic than *n*-octanol and can accommodate linear alkyl chains of ≤6 carbons. Hydrophobic interactions provide a total binding energy of ≈10 kJ/mol. Specificity for the aldehyde substrate is achieved through large decreases in apparent K_m (≈100-fold) and smaller but significant increases in turnover number (≈5-fold). We observed up to 250-fold preference of xylose reductase for reaction with pyridine carbaldehydes, 4-nitro-benzaldehyde, and α-oxo-aldehydes over reaction with D-xylose, perhaps reflecting a secondary role of this enzyme in detoxication metabolism of reactive endogenous aldehydes and compounds of xenobiotic origin.

Key words: detoxication metabolism, hydrogen bonding, hydrophobicity, specificity, substrate-binding site.

Abbreviations: AKR, aldo-keto reductase; hAR, human aldose reductase; XR, xylose reductase; CrfXR, XR from *Cryptococcus flavus;* CtXR, XR from *Candia tenuis*; ds-XR, dual NADH/NADPH-specific XR; ms-XR, NADPH-specific (monospecific) XR. Enzymes: Xylose reductase, aldose reductase [alditol:$NAD(P)^+$ 1-oxidoreductase; EC 1.1.1.21].

Xylose is the major constituent monosaccharide of the heteropolysaccharide hemicellulose, the second most abundant carbohydrate polymer in nature. It represents an important renewable resource for production of chemicals and fuels, but is not well utilized at the present time. Microbial metabolism of xylose has, therefore, aroused much interest in respect to its manipulation and enhancement of its efficiency (*1*, *2*). Enzymes responsible for the initial steps of xylose assimilation are obviously important targets for altering and improving the metabolic capabilities of micro-organisms that are relevant for application in the food and biotech industries (*3*).

Xylose reductase [alditol:$NAD(P)^+$ 1-oxidoreductase; XR, EC 1.1.1.21] is the first enzyme of the catabolic pathway for xylose in fungi. It binds the open-chain free aldehyde form of xylose (*4*) and catalyzes reduction of the C1 carbonyl group, yielding xylitol. XRs can be classified according to co-substrate specificity into a major group of NADPH-specific enzymes (ms-XR), and another, smaller group of enzymes (ds-XR) that can utilize both NADPH and NADH with physiological catalytic efficiencies. A clear bias in the literature towards the dual NADPH/NADH-specific XRs probably reflects the application of fungal xylose metabolism in xylose fermentation by ethanologenic yeasts, in which NADH-linked XR activity is essential (*5*, *6*). However, this leaves the large NADPH-specific group of XRs not well characterized. Relationships of ms-XRs with ds-XRs and structurally related oxidoreductases of the aldo-keto reductase (AKR) superfamily (*7*) have not been conclusively defined on the basis of a rigorous comparison of the corresponding substrate-

*To whom correspondence should be addressed. Tel: +43-316-873-8400, Fax: +43-316-873-8434, E-mail: bernd.nidetzky@tugraz.at

binding pockets via analysis of specificity (*8*). That has been a major goal of the present work.

Like many other AKR enzymes (*9*, *10*) XRs show a broad *in-vitro* substrate specificity (*11–13*). Aside from the canonical substrate xylose, they are capable of reducing a number of different aldehydes whose non-reacting parts represent a wide range of structural scaffolds (*8*, *11*, *12*). In consideration of the apparently well-defined role of XR in fungal physiology, specificity more obviously primed for reaction with xylose might be anticipated. A significant question is, therefore, how substrate specificities and other catalytic properties of ds-XR and ms-XRs reflect evolution of the basic $(\beta/\alpha)_8$ AKR fold towards accomplishment of a given main task in central catabolism and, perhaps, other secondary roles. It is noteworthy that xylose is a reasonably good substrate of many AKR enzymes (*14*) including different reductases of fungal origin. A functional genomics study of *Saccharomyces cerevisiae* AKRs has shown that three out of the six open-reading frames present in the genome encode proteins that are enzymatically active with xylose (*15*). In spite of this, the organism cannot assimilate xylose efficiently. Although, of course, the problem of fungal xylose utilization is complex and cannot be reduced simply to the prevalence of a functional reductase, it is clear from the current state of knowledge that XR-specific features of AKR structure and function still need to be brought into focus.

A literature survey revealed that although the natural habitats for many basidiomycete fungi are potential sources of xylose, published studies have focused completely on XRs from strains belonging to the phylum *Ascomycota* (*e.g.*, *11*, *16–19*). Therefore, we turned our attention to the phylum *Basidiomycota* and chose *Cryptococcus flavus* as a wild-type strain producing significant levels of ms-XR activity during growth on xylose (M.P and N.B., unpublished results). Here, we describe purification of *Cr. flavus* ms-XR (CrfXR) and report a detailed characterization of its substrate specificity. The results reveal that the substrate-binding pockets of CrfXR and ds-XR from the ascomycete fungus *Candida tenuis* (CtXR), a representative XR whose structure and mechanism have been described (*20*, *21*), are very similar overall. Clear differences between the two enzymes are brought to light upon comparison of specificities for reduction of non-carbohydrate aldehydes. High catalytic efficiencies of CrfXR for reduction of very reactive, endogenous and xenobiotic aldehydes point to a possible secondary role for the NADPH-dependent enzyme in detoxication metabolism.

EXPERIMENTAL PROCEDURES

Materials—All chemicals were of the highest purity available and obtained from Sigma-Aldrich or Fluka. Materials for electrophoresis and protein chromatography were purchased from Amersham Pharmacia Biotech. The dye Procion Red H-8B (color index Red 31) was from ICI Chemicals. 2-Keto-D-xylose, 2-keto-D-glucose, and 2-keto-D-allose were synthesized using pyranose-2-oxidase-catalysed oxidation of the corresponding aldoses, as described elsewhere in more detail (*22*), and kindly provided by Prof. D. Haltrich (Institute of Food Technology, BOKU, Austria). 2,3-Diketo-D-glucose was synthesized enzymatically using pyranose dehydrogenase, essentially as reported in a recent publication (*23*), and was a gift of Dr. J. Volc (Institute of Microbiology, Academy of Sciences, Prague, Czech Republic).

Organism and Growth Conditions—The strain *Cryptococcus flavus* (HB402) was obtained from a fungal culture collection maintained at the Institute of Applied Microbiology of the University of Agricultural Sciences in Vienna, Austria. Its natural habitat was the intestine of a termite of the genus *Mastotermes* (*24*). For production of CrfXR, the organism was grown in a 20-liter bioreactor containing media composed of 20 g/liter D-xylose, 4 g/liter yeast extract, and 4 g/liter peptone from casein (enzymatic digest), and supplemented with 0.5 g/liter $MgSO_4$. Dissolved oxygen concentration (20% saturation), pH (4.5), and temperature (25°C) were maintained at constant levels. At the end of the exponential growth phase, which was typically after 24 h of cultivation, fungal biomass was harvested by centrifugation at 10,800 ×*g* and 4°C. Approximately 11 g of dry cell mass per liter of medium was obtained. Washed cells were disrupted with a continuously operated ball mill (Dynomill, KDL Bachofen AG, Switzerland) using glass beads of 0.25 to 0.5 mm in diameter, an average residence time of 8 minutes, and a maximum temperature of 10°C. The crude cell extract was obtained after removing cell debris by ultracentrifugation at 100,000 ×*g* (30 min, 4°C). It was stored at –70°C prior to further use.

Protein Purification—Elution column chromatography was carried out at room temperature with an Äktaexplorer 100 system using absorbance at 280 nm for detection of eluted protein. Prior to use, all buffers were filtered through a 0.45 μm filter and degassed with a vacuum pump.

Hydrophobic Interaction Chromatography—Ligand screening for hydrophobic interaction chromatography (HIC) was carried out with a PIKSII kit (Amersham Pharmacia Biotech) according to the supplier's instructions. This led to the selection of phenyl-Sepharose. For purification of CrfXR, a 5 cm × 8 cm column (XK 50; Amersham Pharmacia Biotech) was filled with 150 ml of phenyl-Sepharose CL-4B high sub fast flow and packed with 20% ethanol at 10 ml/min. The column was equilibrated with 600 ml of 1 M $(NH_4)_2SO_4$ in 50 mM potassium phosphate buffer, pH 7.0. The crude extract was brought to 1 M $(NH_4)_2SO_4$ with cold 4 M $(NH_4)_2SO_4$ solution in 50 mM potassium phosphate buffer, pH 7.0. About 10 mg of protein/ml of gel was loaded on the column using a flow rate of 10 cm/h. Elution was performed at 20 cm/h (6 ml/min) in a linear $(NH_4)_2SO_4$ gradient. XR was eluted at 35 to 45% salt.

Concentration and Buffer Exchange—XR-containing fractions were pooled and concentrated by ultrafiltration (Amicon 8200, equipped with a PM 10 filter, cut off 10 kDa) at 4°C with 4 bar N_2 pressure. Buffer exchange was performed with a Sephadex G-25 fine HiPrep 26/10 column (flow rate 15 ml/min) to 10 mM potassium phosphate buffer, pH 7.0.

Dye-Ligand Chromatography—Procion Red H-8B (reactive Red 31) was immobilized on Sepharose CL-4B as described elsewhere in detail (*25*). A 5 cm × 15 cm XK 50 column was filled with 300 ml of Red 31 gel, packed with

Table 1. **Purification of xylose reductase from *Cryptococcus flavus*.**[a]

Purification step	Total activity (U)	Specific activity (U/mg)	Purification (fold)	Yield (%)
Crude extract	620	1.1	1	100
$(NH_4)_2SO_4$-addition	560	1.2	1.1	91
Phenyl-HIC with 25% $(NH_4)_2SO_4$	490	6.5	5.9	79
Concentration and buffer exchange	350	6.5	5.9	56
Red 31 affinity chromatography	180	21	19	29

[a]Results are based on processing 30 g of wet fungal biomass.

20% ethanol at a flow rate of 6 ml/min and equilibrated with 1500 ml of 10 mM potassium phosphate buffer, pH 7.0. The concentrated enzyme solution was applied to the column (0.2 mg protein/ml gel) at a flow of 7 cm/h. Elution was performed with a step gradient of 0 to 2 M NaCl at a flow rate of 20 cm/h (6 ml/min). Under these conditions, XR was eluted at 2 M NaCl. The active fractions were combined and concentrated to about 5 mg/ml, the buffer was changed to 50 mM potassium phosphate buffer, pH 7.0, as described above and the enzyme preparation was stored in aliquots at –70°C prior to use.

Assays and Kinetics—All spectrophotometric measurements were performed with a Beckman DU-650 instrument. Unless mentioned otherwise, 50 mM potassium phosphate buffer, pH 7.0, was used; and initial rates were recorded at 340 nm and 25°C in measuring the oxidation of NADPH or the reduction of $NADP^+$. Enzyme solutions were diluted as required to ensure constancy of Δ(absorbance at 340 nm)/Δ(time) for reaction times of at least 1 min. Under these conditions and using 700 mM xylose and 200 μM NADPH as the substrates, one unit of XR activity corresponds to 1 μmol NADPH oxidized per minute. Kinetic parameters for D-xylose reduction and xylitol oxidation were obtained from initial-rate data measured at six constant levels of NADPH (3.3–170 μM) and $NADP^+$ (10–500 μM) and using xylose and xylitol as the varied substrates, respectively. Apparent kinetic parameters for aldehyde reduction were obtained from initial-rate data recorded at a constant NADPH concentration of 220 μM NADPH, which is fully saturating at the steady state (see later). Protein concentrations were determined with the Bio-Rad protein assay referenced against standard solutions with known BSA concentrations of between 0.1 and 1.0 mg/ml.

Quaternary Structure, Molecular Mass and Isoelectric Point—The molecular mass of CrfXR subunit was determined by using SDS/PAGE and matrix assisted laser-desorption/ionization MS (MALDI-MS) as described elsewhere (*26*). Column-sizing experiments were used to deduce the molecular mass of functional CrfXR. To validate results of the analysis, two different gel filtration columns, Superose 12 HR 10/30 and Superdex 75 HR 10/30 (both from Amersham Pharmacia Biotech), were used. Purified CrfXR (≈0.3 mg/ml in a volume of 500 μl) was applied onto each column equilibrated with 50 mM potassium phosphate buffer, pH 7.0, containing 200 mM NaCl. Elution was carried out at a constant flow rate of 0.3 ml/min. Calibration for molecular mass determination was performed by using the following standard proteins: cytochrome *c* (12.4 kDa), myoglobin (17.6 kDa), α-lactoglobulin (35 kDa), egg albumin (43 kDa), BSA (67 kDa), hexokinase (100 kDa), and aldolase (158 kDa). The pI of purified CrfXR was determined by IEF PAGE using precast gels in the pH ranges 3.0–9.0 and 4.0–6.5, and an isoelectric calibration kit (all from Amersham Pharmacia Biotech).

RESULTS AND DISCUSSION

Purification and Structural Properties of CrfXR—Crude cell extracts of *Cr. flavus* grown on xylose contained approximately 9 U/ml NADPH-linked XR activity with a specific activity of 1.1 U/mg of protein. No activity was detectable using NADH. XR activity was purified by a two-step procedure (Table 1). Analysis by SDS PAGE demonstrates apparent homogeneity of the isolated protein (Fig. 1).

Staining for XR activity after non-denaturing electrophoresis revealed that the protein band was enzymatically active and required NADP(H) as co-substrate (not shown). Purified CrfXR eluted as single protein peak in high-resolution anionic exchange chromatography on a MonoQ column and gel permeation chromatography on a Superose 12 column, suggesting the absence of substantial structural microheterogeneity due to posttranslational modifications. MALDI-TOF MS analysis yielded a value of 35,322 Da for the molecular mass of CrfXR subunit. The analysis by SDS–PAGE in Fig. 1 gave a closely similar value of 35,000 ± 1,000 Da. Functional molecular masses of 58,000 ± 4,000 Da, and 62,000 ± 4,000 Da have

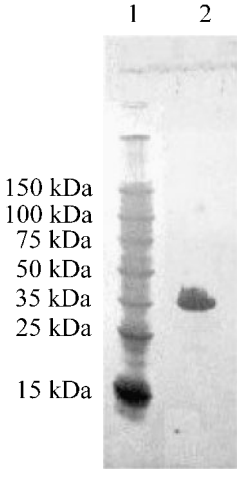

Fig. 1. **Purification of CrfXR documented by SDS PAGE.** Lane 1, SDS standard proteins (Sigma); lane 2, CrfXR after Red 31 chromatography. Electrophoresis was carried out with an Amersham Pharmacia Biotech Phast-System using Phast Gel Gradient 8–25 and silver staining for visualization of protein bands.

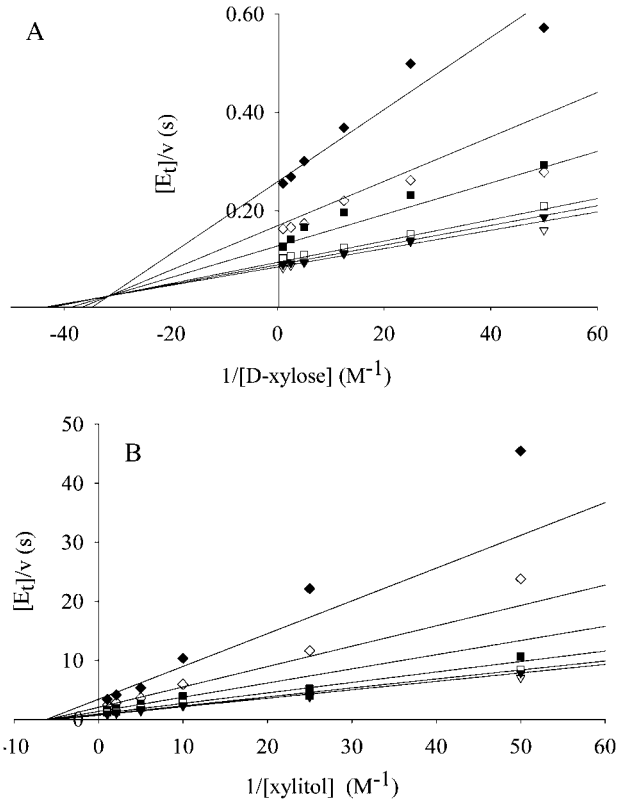

Fig. 2. **Double-reciprocal plot from initial-rate measurements for NADPH-dependent reduction of xylose (A) and NADP$^+$-dependent oxidation of xylitol (B) by CrfXR.** Observed rates were related to the total concentration of 35-kDa enzyme subunits present (E_t). In panel A, NADPH concentrations were 3.3 μM (full diamonds), 6.7 μM (open diamonds), 12.7 μM (full squares), 46 μM (open squares), 75 μM (full triangles), and 170μM (open triangles). In panel B, NADP$^+$ concentrations were 10 μM (full diamonds), 20 μM (open diamonds), 40 μM (full squares), 100 μM (open squares), 250 μM (full triangles), 500 μM (open triangles). Lines are calculated from a non-linear fit of the data to Eq. 2.

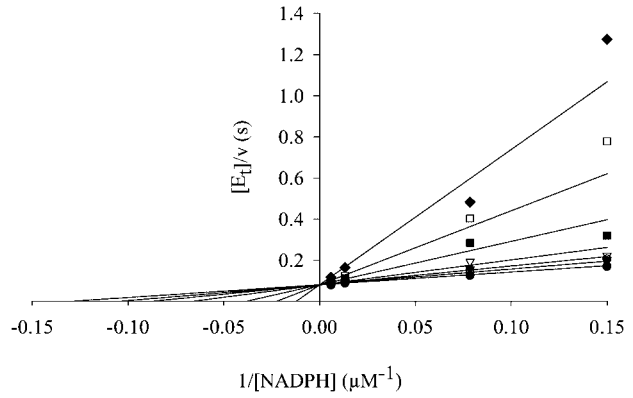

Fig. 3. **Double-reciprocal plot from initial-rate measurements for NADPH-dependent reduction of xylose by CrfXR in the absence and presence of NADP$^+$.** Observed rates were related to the total concentration of 35-kDa enzyme subunits present (E_t). The NADP$^+$ concentrations were 5 μM (full diamonds), 10 μM (open diamonds), 20 μM (full squares), 50 μM (open squares), 100 μM (full triangles), and 200 μM (open circle). The concentration of xylose was constant and saturating (700 mM). Lines are calculated from a non-linear fit of the data to a single substrate Michaelis-Menten equation expanded to incorporate inhibition by a competitive inhibitor.

been determined by column-sizing experiments using a Superose 12 and Superdex 75 column, respectively. The results suggest that CrfXR exists exclusively as dimer in solution, and the dimer is probably composed of identical subunits.

Two further outcomes of CrfXR purification are worth noting. First, fractionation of the cell extract did not reveal proteins having NADPH- or NADH-linked XR activity other than the one purified, essentially ruling out formation of another major XR by *Cr. flavus*. Multiple forms of XR have been found in other fungi (*27–29*). Second, establishing an efficient procedure for isolation of CrfXR required that dye-ligand chromatography not be used as the first purification step. Considering our suggestions for a procedure generally applicable to XR purification (*25*), 20 triazine dyes representing a wide range of protein-binding capacity were tested as potential biomimetic ligands, but no detectable capture of CrfXR from crude cell extract was found. Partially purified enzyme showed practically useful binding to a Red 31-Sepharose CL-4B column. However, the capacity of the column for binding CrfXR was just one tenth of that for binding CtXR (*25*).

Steady-State Kinetic Analysis for Xylose Reduction and Xylitol Oxidation—Initial-rate measurements were carried out in the direction of xylose reduction under conditions of the standard enzyme assay but using either NADPH or NADH at a constant level of 200 μM. Within the limit of detection of the assay, which was estimated to be approximately 0.02–0.05% of the rate recorded with NADPH, CrfXR was inactive with NADH as co-substrate. Therefore, a detailed steady-state kinetic analysis was carried out for the physiological reaction, D-xylose + NADPH + H$^+$ ↔ xylitol + NADP$^+$, at pH 7.0 and 25°C. Double reciprocal plots for initial-rate data recorded in forward and reverse directions of the reaction are displayed in Figs. 2, A and B.

Both graphs show a characteristic "intersecting line" pattern, which is indicative of a sequential bi-substrate reaction in which a ternary enzyme-substrate complex must be formed before any product is released. A steady-state ordered bi-bi kinetic mechanism, in which NADPH binds first and NADP$^+$ leaves last appears to be typical of many AKR oxidoreductases (*e.g.*, *14*, *30*) including CtXR (*21*). In this mechanism, NADPH and NADP$^+$ compete for binding to free enzyme. NADP$^+$ was tested as inhibitor of CrfXR-catalyzed reduction of xylose using varied concentrations of NADPH at a constant saturating level of substrate. The double reciprocal plot of the experimental data is shown in Fig. 3 and demonstrates competitive inhibition of NADP$^+$ against NADPH.

Though it is not a proof, this result provides supporting evidence that analysis of kinetic data can be made with assumptions implied in Scheme 1 and by using Eq. 1,

$$v = k_{cat}[E][A][B]/\{K_{iA}K_B+K_B[A]+K_A[B]+[A][B]\} \quad (1)$$

Table 2. **Steady state kinetic parameters for CrfXR.**[a]

D-xylose reduction		xylitol oxidation	
k_{catR} (s^{-1})[b]	15.5[c]	k_{catO} (s^{-1})[b]	1.0
K_{xylose} (mM)	21.4	$K_{xylitol}$ (mM)	202
K_{NADPH} (μM)	7.1	K_{NADP+} (μM)	41.4
K_{iNADPH} (μM)	10.5[d]	K_{iNADP+} (μM)	31.3[d] (20.8)[e]
K_{eq}	446[f] (528)[g,d]		

[a]Initial-rate data were obtained in 50 mM potassium phosphate buffer, pH 7.0, and at 25°C; parameters are the results of non-linear fits of the data shown in Fig. 2, A and B, to Eq. 1; [b]k_{catR}, turnover number for reduction of xylose; k_{catO}, turnover number for oxidation of xylose; [c]unless indicated otherwise, calculated standard deviations for the fitted estimates were smaller than 12% of the reported values; [d]calculated standard deviations smaller than 20%; [e]obtained from fits of data in Fig. 3 to the equation for competitive inhibition; [f]calculated from the Haldane relationship for an ordered bi-bi mechanism, $K_{eq} = (k_{catR}/K_{xylose})K_{iNADP}/\{(k_{catO}/K_{xylitol})K_{iNADPH}\}$; [g]experimental equilibrium constant at pH 7.0, calculated according to K_{eq} = [$NADP^+$] [xylitol]/([NADPH] [xylose]) for the reaction, D-xylose + NADPH + H+ ↔ xylitol + $NADP^+$.

where v is the initial rate, K_A and K_B are Michaelis constants for coenzyme and substrate, [A] and [B] are concentrations of coenzyme and substrate, and K_{iA} is the apparent dissociation constant of the binary complex between CrfXR and coenzyme.

Kinetic parameters for xylose reduction and xylitol oxidation were obtained from non-linear fits of initial-rate data to Eq. 1 using the Sigma Plot 2000 program and are summarized in Table 2. The internal consistency of the kinetic parameters was checked by using the Haldane relationship for an ordered bi-bi kinetic mechanism, as shown in the legend to Table 2. The calculated value of 446 for the equilibrium constant (K_{eq}) at pH 7.0 and 25°C agrees well with the experimentally observed value of 528 at this pH. Similar values for K_{iNADP+} were obtained from extrapolations to either a very low level of NADPH in inhibition experiments carried out at saturating concentration of xylose or very low concentrations of both reactants so that only the free enzyme was present (Eq. 1). The result is as expected if $NADP^+$ bound only to the free CrfXR (Scheme 1). Comparison of $K_{iNADP(H)}$ values indicates approximately 2- to 3-fold tighter apparent binding of NADPH than $NADP^+$. Considering the normally high ratio of intracellular concentrations of NADPH and $NADP^+$, CrfXR should generally be primed for reductive metabolism, and product inhibition by $NADP^+$ should be hardly significant. Comparison of k_{cat}/K_B values reveals a large, approximately 150-fold preference for reduction of xylose over oxidation of xylitol. This result reinforces the conclusion of a completely unidirectional function of CrfXR in xylose metabolism.

Characterization of the Substrate Binding Site of CrfXR—General: The unusually broad substrate specificity of many AKR members including the xylose reductases could be explained in two different ways: (i) the

$$E + A \underset{k_2}{\overset{k_1}{\rightleftharpoons}} EA + B \underset{k_4}{\overset{k_3}{\rightleftharpoons}} EAB \underset{k_6}{\overset{k_5}{\rightleftharpoons}} EPQ \underset{k_8}{\overset{k_7}{\rightleftharpoons}} EQ + P \underset{k_{10}}{\overset{k_9}{\rightleftharpoons}} E + Q$$

Scheme 1. **Tentative kinetic mechanism of CrfXR.** E is the enzyme, A is NADPH, B is xylose, P is xylitol and Q is $NADP^+$. k_1 to k_{10} are rate constants.

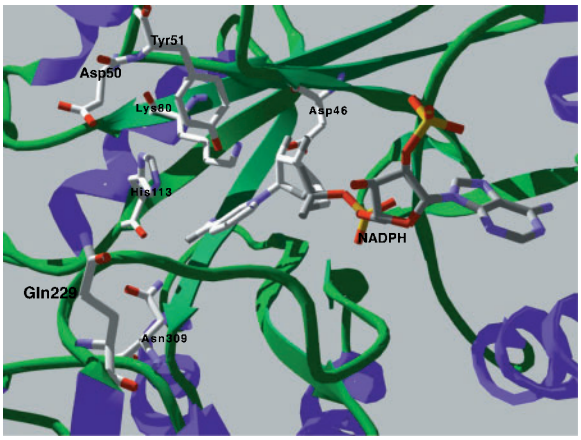

Fig. 4. **The substrate binding site of *Candida tenuis* XR having NADP(H) bound (*20*).** The figure has been drawn with the aim of emphasizing the few polar groups that are potentially available for interactions with sugar hydroxyls. The active-site tetrad Tyr-51/Lys-80/Asp-46/His-113 is also shown. On the basis of this figure, the comparison of CrfXR and CtXR with regard to k_{cat}/K_m values for reaction with sugars is relevant, considering the limited number of possible hydrogen bonds.

topology of the substrate binding site, particularly the position of the loops that form the sides of the apolar cleft leading to the active site, is rather flexible, such that the exact binding mode is dependent on structural features of the non-reacting portions of the aldehyde; (ii) the binding site is essentially indiscriminate, because no significant transition-state stabilization energy is derived from non-covalent interactions with the substrate. Studies of ligand recognition and catalysis by α-hydroxysteroid dehydrogenase, a well-characterized AKR member, have revealed elegantly that different binding modes for substrates do occur within the same binding pocket (*31*). Likewise, the substrate binding site of *C. tenuis* XR is not indiscriminate and capable of utilizing hydrogen bonding to bring about specificity for xylose (*13*). This is illustrated in Fig. 4, which points out the few polar residues in the substrate binding pocket of CtXR. Therefore, characterization of the substrate binding site of CrfXR required that different series of structurally related aldehydes be compared as substrates of the enzyme and that structural features leading to high k_{cat}/K_m, high k_{cat}, or low K_m (which is an apparent Michaelis constant) be deduced in a systematic fashion. For steady-state kinetic measurements, we chose aldehydes differing in hydrophobic and hydrogen bonding capabilities with the enzyme-NADPH complex. Furthermore, a number of highly reactive aldehydes were tested as substrates to evaluate the potential of CrfXR to protect the cell against xenobiotic and endogenous aldehydes.

Aliphatic aldehydes as substrates of CrfXR and hydrophobic bonding effects—Aldehydes of the form R-CHO, where R is an unbranched or branched alkyl chain, were used as substrates of NADPH-dependent reduction by CrfXR. Initial rates were fitted to the Michaelis-Menten equation and apparent kinetic parameters for NADPH-dependent enzymic reduction are summarized in Table 3. The value for k_{cat}/K_m increases approximately 60-fold as R increases in size and hydrophobicity from -CH_2-CH_3 to

Table 3. **Apparent kinetic parameters of CrfXR for NADPH-dependent reduction of aliphatic aldehydes of the form R-CHO, where R is the alkyl chain.**

Alkyl chain R	k_{cat} (s^{-1})	K_m (mM)	k_{cat}/K_m (mM^{-1} s^{-1})	$-\Delta\Delta G_{trans}$ (*n*-octanol→H_2O)[a] (kJ/mol)	$-\Delta\Delta G^{\#}$ (kJ/mol)
-CH_3	15.0[b]	35	0.44	—	—
-CH_2-CH_3	12.9	34	0.38	5.6	0.0
-$(CH_2)_2$-CH_3	13.3	7.9	1.7	8.4	3.7
-$(CH_2)_3$-CH_3	14.4	2.2	6.4	11	7.0
-$(CH_2)_4$-CH_3	14.0	0.72	19	14	9.8
-$(CH_2)_5$-CH_3	14.8	0.61	24	17	10
-$(CH_2)_6$-CH_3	14.3	2.0	7.3	20	7.3
-$(CH_2)_7$-CH_3	14.2	2.2	6.6	22	7.1
-CH-$(CH_3)_2$	13.7	8.3	1.7	7.3	3.7
-CH(CH_3)-CH_2-CH_3	12.8	2.7	4.8	10	6.3
-CH_2-CH$(CH_3)_2$	14.6	9.2	1.6	10	5.5
-CH(CH_3)-$(CH_2)_2$-CH_3	6.2	1.8	3.5	13	3.6
-CH-$(C_2H_5)_2$	4.3	3.2	1.3[c]	13	3.1
-C-$(CH_3)_3$	11.0	46	0.24	8.9	–1.1

[a]Incremental Gibbs free energy of transfer of the group R from *n*-octanol to water, calculated by using the relationship $\Delta\Delta G_{trans} = -2.303\ RT\pi$ where π is the hydrophobicity constant of *R*, relative to the hydrogen atom (*32*); [b]unless indicated otherwise, standard deviation was smaller than 18% for all values; [c]standard deviation was 32%. The NADPH concentration was 220 μM and saturating (≈31 × K_{NADPH}). Initial rates were determined in 50 mM potassium phosphate buffer, pH 7.0, and at 25°C. $\Delta\Delta G^{\#}$ was calculated according to Eq. 2.

-$(CH_2)_5$-CH_3, suggesting that the substrate binding site can accommodate the aldehyde group and an alkyl chain of six carbon atoms in length. The value of k_{cat} appears to be hardly affected by structural changes of R, perhaps indicating that rate limitation for k_{cat} is due to steps outside the sequence of steps contributing to k_{cat}/K_m. Therefore, the observed increases in the specificity constant are entirely due to decreases in apparent K_m by about the same factor. Adding more than five methylene groups leads to decreases in k_{cat}/K_m to approximately one third of the maximum value. When substrates with branched and unbranched alkyl chains are compared on the basis of similar side chain hydrophobicity or the same number of carbons, k_{cat}/K_m values are consistently smaller for branched substrates, perhaps as a result of steric hindrance. Maximum transition-state stabilization energy derived from hydrophobic bonding with R is estimated to be approximately 10 kJ/mol, comparing catalytic efficiencies for reductions of hexanal and propanal by using Eq. 2,

$$\Delta\Delta G^{\#} = -RT \ln [(k_{cat}/K_m)_{R\text{-}CHO}/(k_{cat}/K_m)_{propanal}] \qquad (2)$$

where *R* is the gas constant in J/(K mol) and *T* is the temperature in K. When the values of $\Delta\Delta G^{\#}$ are plotted against the incremental Gibbs free energy of transfer of *R* from *n*-octanol to water ($\Delta\Delta G_{trans}$ values in Table 3), a linear relationship is obtained for the range of R from -CH_2-CH_3 to -$(CH_2)_5$-CH_3 (not shown). Fit of the data to a straight line yielded a slope value of 1.15 and a good correlation coefficient of 0.996. Therefore, the result implies that the substrate-binding pocket of CrfXR is approximately 1.15 times more hydrophobic than n-octanol and, upon comparison with literature data, 1.2-fold and 2.1-fold less hydrophobic than aldehyde binding sites of CtXR (*13*) and human aldose reductase (hAR) (*9*), respectively. Probably because of unfavorable steric effects, most of the branched aldehydes did not fit into the correlation, $\Delta\Delta G^{\#}$ *vs.* $\Delta\Delta G_{trans}$. Correlations of log (k_{cat}/K_m) values for CrfXR-catalyzed reduction of R-CHO in Table 3 with corresponding log (k_{cat}/K_m) values reported for CtXR (*13*) and hAR (*9*) were linear (not shown), suggesting similarity among the three enzymes in regard to the mode of binding aliphatic aldehydes.

Polyhydroxylated aldehydes (sugars) as substrates of CrfXR and hydrogen bonding effects—Apparent kinetic parameters for NADPH-dependent reduction of a series of different aldoses and derivatives thereof were determined to characterize the positioning of carbohydrates at

Table 4. **Apparent kinetic parameters of CrfXR for NADPH-dependent reduction of different pentoses.**

Substrate	(%)[a]	k_{cat} (s^{-1})	K_m[b] (μM)	k_{cat}/K_m[b] (μM^{-1} s^{-1})	$-\Delta\Delta G^{\#}$ (kJ/mol)
D-xylose	0.02	16.3[c]	3.6	4.5	16
L-arabinose	0.03	12.5	4.2	3.0	15
D-ribose	0.05	12.4	22	0.56	11
2-deoxy-D-ribose	0.01	2.5	53	0.047	4.9
L-lyxose	0.03	11.3	27	0.42	10
D-lyxose	0.03	4.7	82	0.057	5.4
pentanal	100	14	2200	0.0066	0.0

[a]Percentage of free aldehyde present in aqueous solution of the sugar (*33*); [b]corrected for free aldehyde in solution; [c]standard deviations for k_{cat} and K_m were smaller than 10% and 16% of the reported values, respectively. The NADPH concentration was 220 μM and saturating (≈31 × K_{NADPH}). Initial rates were determined in 50 mM potassium phosphate buffer, pH 7.0, and at 25°C. $\Delta\Delta G^{\#}$ was calculated according to Eq. 2.

Table 5. **Apparent kinetic parameters of CrfXR for NADPH-dependent reduction of different hexoses.**

Substrate	(%)[a]	k_{cat} (s^{-1})	K_m[b] (μM)	k_{cat}/K_m[b] (μM^{-1} s^{-1})	$-\Delta\Delta G^{\#}$ (kJ/mol)
L-idose	0.1[c]	24[c]	3.2	7.5	15
D-galactose	0.02	9.6	10	0.94	9.6
2-deoxy-D-galactose	0.03	6.7	170	0.039	1.8
D-glucose	0.0024	5.0	2.5	2.0	11
2-deoxy-D-glucose	0.008	5.8	19	0.30	6.8
D-mannose	0.005	8.4	34	0.25	6.3
D-allose	0.01	n.d.[d]	n.d.[d]	0.58[e]	8.4
hexanal	100	14	720	0.019[e]	0.00

[a]Percentage of free aldehyde present in aqueous solution of the sugar (*33*); [b]corrected for free aldehyde in solution; [c]standard deviations for k_{cat} and K_m were smaller than 10% and 19%, respectively; [d]n.d., not determined; [e]catalytic efficiency was derived from the part of the Michaelis-Menten curve where the reaction rate is linearly dependent on the aldehyde concentration. The NADPH concentration was 220 μM and saturating (≈31 × KNADPH). Initial rates were determined in 50 mM potassium phosphate buffer, pH 7.0, and at 25°C. $\Delta\Delta G^{\#}$ was calculated according to Eq. 2.

the substrate-binding site of CrfXR and identify interactions with individual hydroxy groups that make an important contribution to specificity. Results are summarized in Tables 4 and 5 and reveal a clear dependence of k_{cat}/K_m and k_{cat} on the configuration of hydroxy groups in pentose and hexose substrates. The variation in catalytic efficiency across the pentose series is approximately 100-fold and reflects a 6.5-fold variation of k_{cat} and a 20-fold variation in apparent K_m.

CrfXR displays highest specificity constants for reactions with the physiological substrate D-xylose, and L-idose. To estimate the maximum transition-state stabilization energy derived from productive bonding with hydroxy groups, we use Eq. 2 and compare k_{cat}/K_m values for reduction of the preferred pentose and hexose with catalytic efficiencies for reactions with pentanal and hexanal, respectively. Differential binding energy stabilizing the transition state for NADPH-dependent reduction of sugars is approximately 15–16 kJ/mol. Comparisons of k_{cat}/K_m values of D-ribose, D-galactose, or D-glucose with the corresponding 2-deoxy derivative shows clearly that interactions with the C-2(*R*) hydroxy group contribute most, approximately 5–8 kJ/mol, to transition-state stabilization. A hydrogen bond between this hydroxy group and an uncharged donor or acceptor group on the enzyme could provide such a net amount of binding energy. Comparisons of sugars having *R*-configured C-2 with the corresponding C-2 epimers (D-xylose *vs.* D-lyxose; D-glucose *vs.* D-mannose) indicate that losses of transition-state stabilization energy in the C-2(*S*) substrates and in the 2-deoxy substrates are similar. Therefore, aldose substrates having *R*-configured C-2 are preferred over their C-2 epimers, clearly because the substrate binding site of CrfXR provides favorable interactions with the C-2(*R*) hydroxy group which are lacking in C-2(*S*) substrates. Comparison of kinetic parameters for reductions of D-ribose and 2-deoxy-D-ribose shows that replacement of the 2-OH by hydrogen leads to a 5-fold decrease in the value of k_{cat} and a 12-fold decrease in k_{cat}/K_m. The result appears to be at variance with the observation in Table 3 that an approximately 50-fold variation in specificity constant across a series of n-alkyl aldehydes is accompanied by essentially no change in the value of k_{cat} for the same substrates. These apparently inconsistent results can be reconciled by assuming that interactions mediated by C-2(*R*) hydroxy group have a role in preventing non-productive binding with the aldose substrate, which will lead to a decrease in k_{cat} by the fraction of enzyme productively bound.

Results in Table 4 reveal that the hydroxy group at C-3 also contributes to stereochemical selection of polyhydroxylated substrates. Comparison of specificity constants for reactions with D-xylose and D-ribose as well as L-arabinose and L-lyxose indicates that the *S* configuration is preferred at this carbon. The differential binding energy is estimated to be 5 kJ/mol, and this value could reflect productive bonding with the C-3(*S*) hydroxy group or non-favorable interactions with C-3(*R*) hydroxy group. Interactions at C-4 appear to have little effect on specificity, because k_{cat}/K_m values for reactions with D-xylose and L-arabinose, D-ribose and L-lyxose, and D-glucose and D-galactose are very similar. Differential binding energies smaller than *RT* are obtained upon comparison of these substrate pairs. Hydroxy groups at C-5 and C-6 have been shown not to make a significant contribution to specificity of CrfXR (*4*). Interestingly, therefore, 2-deoxy-D-ribose, which according to the above analysis of CrfXR stereoselectivity should be among the poorest pentose substrates of the enzyme, was reduced with a catalytic efficiency significantly greater than the specificity constant for reduction of pentanal, the n-alkyl aldehyde having the corresponding number of carbons. This observation arguably reflects slightly different binding modes for carbohydrates and hydrophobic aldehydes at the substrate-binding site of CrfXR. It sets an approximate limit of ≈1–2 *RT* to the estimation of a differential binding energy between the two substrate series in Tables 3–5. However, it reveals that, unexpectedly, the hydrophobic nature of the aldehyde binding site of CrfXR does not strongly disfavor binding of polar carbohydrate substrates, in spite of the very limited number of attractive interactions that were clearly identifiable through Tables 4 and 5. Correlation of log (k_{cat}/K_m) values for CrfXR-catalyzed reductions in Tables 3–5 with corresponding log (k_{cat}/K_m) values reported for CtXR (*13*) is shown in Fig. 5. A linear relationship with a slope value of 0.90 is obtained, indicating a high degree of similarity among the substrate-binding sites of CrfXR and CtXR overall (*cf.* Fig. 4). However, the correlation coefficient for the straight-line fit in Fig. 5 is only 0.84, and this implies dif-

Table 6. **Apparent kinetic parameters of CrfXR for NADPH-dependent reduction of potentially toxic aldehydes.**

Substrate	k_{cat} (s^{-1})	K_m (mM)	k_{cat}/K_m (M^{-1} s^{-1}) × 10^{-3}
α-oxo-aldehydes			
glyoxal	17.5[a]	21	0.81 (5.0)[b]
methylglyoxal	16.9	0.96	18 (300)[b]
2-keto-D-xylose	20.4	2.5	8.2[c]
2-keto-D-glucose	23.8	3.2	7.4[c] (9.2)[b]
2,3-diketo-D-glucose	23.9	5.7	4.2[c]
2-keto-D-allose	25.8[d]	2.7	9.6[c]
xenobiotic aldehydes			
acrolein	21.5	3.3	6.6 (18)[b]
pyridine-2-carbaldehyde	16.2	0.15	110
pyridine-3-carbaldehyde	15.1	0.27	56
pyridine-4-carbaldehyde	17.9	0.075	240
4-nitro-benzaldehyde[e]	29.5	0.13	220 (880)[b]
3-nitro-benzaldehyde[e]	21.4	0.50	42

[a]Unless indicated otherwise, standard deviations for k_{cat} and K_m were smaller than 6% and 18% of the reported values, respectively; [b]Specificity constants for aldose reductase from human skeletal muscle are shown in parenthesis (*10*, *36*); [c]values not corrected for free aldehyde present in aqueous solution; [d]standard deviation for k_{cat}/K_m was smaller than 33%; [e]data from Ref. *8*. The NADPH concentration was 220 μM and saturating (≈31 × K_{NADPH}). Initial rates were determined in 50 mM potassium phosphate buffer, pH 7.0, and at 25°C.

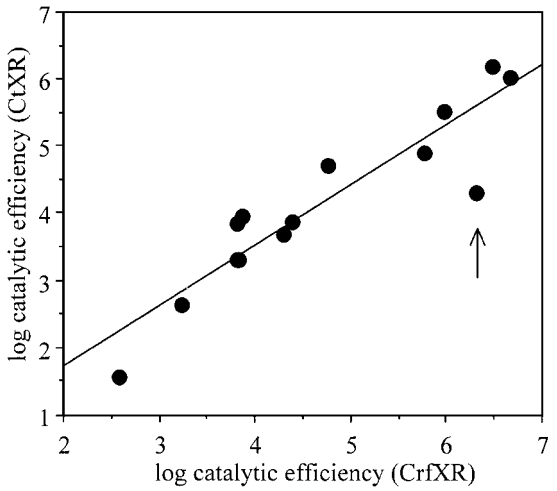

Fig. 5. **Measurement of substrate-binding site similarities among CrfXR and CtXR by correlating catalytic efficiencies for NAD(P)H-dependent reductions of alkyl aldehydes and aldose sugars.** Data for reactions catalyzed by CtXR and CrfXR are taken from Neuhauser *et al.* (*13*) and Tables 3 to 5, respectively. The arrow indicates reduction of D-glucose. The catalytic efficiencies are expressed in M^{-1} s^{-1} and are corrected for free aldehyde in solution.

ferent enzyme-substrate interactions at the level of individual aldehydes. Glucose, which is a good substrate of CrfXR but a poor substrate of CtXR, is an example to this effect (indicated by an arrow in Fig. 5).

Xenobiotic and endogenous aldehydes are good substrates of CrfXR—A possible physiological role of hAR in detoxification metabolism of endogenous aldehydes has been discussed on the basis of the exquisite kinetic properties of this enzyme (*34*). Tight binding of NADPH such that saturation in nucleotide is achieved at all times to generate the reactive binary complex, and low K_m values for a wide range of substrates are key components of hAR function as an efficient broad-spectrum "aldehyde reductase" (*34*). We have determined kinetic parameters for CrfXR-catalyzed reduction of a series of common endogenous and xenobiotic aldehydes to examine whether XR might also function as a detoxification enzyme for certain carbonyl compounds. Results are summarized in Table 6. α-Oxo-aldehydes, which have various carbohydrate-related metabolic origins *in vivo*, are good substrates of CrfXR, even though they all exist almost exclusively (>99.5%) as aldehyde hydrates in aqueous solution (*35*). Methylglyoxal, for example, has been suggested to be a physiological substrate of hAR (*10*, *36*, *37*). On the basis of apparent Michaelis constants uncorrected for aldehyde hydration, they are up to 20-fold better substrates than xylose. Table 6 compares specificity constants of CrfXR and hAR for reduction of selected α-oxo-aldehydes. hAR is generally more efficient than CrfXR, reflecting K_m values that are 10- to 100-fold smaller for the human enzyme. Interestingly, k_{cat}/K_m values for reaction with 2-keto-D-glucose ("glucosone"), a compound possibly relevant in nonenzymatic protein glycation (*38*), are almost identical for human and fungal enzymes.

Acrolein, which has various metabolic origins (*e.g.*, *39*), is reduced by CrfXR and hAR with similar specificity constants. Aromatic aldehydes such as pyridine carbaldehydes and nitro-benzaldehydes are excellent substrates of CrfXR. On the basis of uncorrected K_m values, they gave the highest specificity constants of all carbonyl compounds tested and are up to 250-fold better substrates than xylose. The low K_m values for the heterocyclic substrates are worth noting. Interestingly, very high specificity constants for reduction of pyridine carbaldehydes are not generally found among xylose reductases. Compared to xylose in k_{cat}/K_m terms, CtXR and ms-XR and ds-XR from *Candida intermedia* (*28*) are only 2- to 7-fold more active with pyridine carbaldehyde substrates. Summarizing the data, CrfXR is clearly not designed for a main function in reductive metabolism of potentially toxic aldehydes, because K_m values for substrates are generally high and binding of NADPH is weak. These properties are not consistent with detoxification efficiency (*34*, *10*). However, if we consider the high levels of CrfXR present in the fungal cytosol when the organism grows on xylose as carbon source – a rough estimate based on the specific activity of the enzyme is 5% of the total protein– selected endogenous and xenobiotic aldehydes accumulating to physiological concentrations near 0.1 × K_m could be real targets of CrfXR reductive action. Glucosone and pyridine aldehydes are possible examples.

Financial support from the Austrian Science Funds (FWF project P-15208-MOB) and from the European Commission (EU FAIR CT 96–1098) is gratefully acknowledged. Prof. Dietmar Haltrich and Dr. J. Volc kindly provided purified samples of α-oxo-aldose sugars. Mario Klimacek (Graz) is thanked for the preparation of Fig. 4.

REFERENCES

1. Aristidou, A. and Penttilä, M. (2000) Metabolic engineering applications to renewable resource utilization. *Curr. Opin. Biotechnol.* **11**, 187–198
2. Zaldivar, J., Borges, A., Johansson, B., Smits, H.P., Villas-Boas, S.G., Nielsen, J., and Olsson, L. (2002) Fermentation performance and intracellular metabolite patterns in laboratory and industrial xylose-fermenting *Saccharomyces cerevisiae*. *Appl. Microbiol. Biotechnol.* **59**, 436–442
3. Hahn-Hägerdal, B., Wahlbom, C.F., Gardonyi, M., van Zyl, W.H., Cordero Otero, R.R., and Jonsson, L.J. (2001) Metabolic engineering of *Saccharomyces cerevisiae* for xylose utilization. *Adv. Biochem. Eng. Biotechnol.* **73**, 53–84
4. Nidetzky, B., Mayr, P., Hadwiger, P., and Stütz, A.E. (1999) Binding energy and specificity in the catalytic mechanism of yeast aldose reductases. *Biochem J.* **344**, 101–107
5. van Dijken, J.P. and Scheffers, W.A. (1986) Redox balances in the metabolism of sugars by yeasts. *FEMS Microbiol. Rev.* **32**, 199–224
6. Bruinenberg, P.M., de Bot, P.H.M., van Dijken, J.P., and Scheffers, W.A. (1984) NADH-Linked aldose-reductase: The key to anaerobic alcoholic fermentation of xylose by yeasts. *Appl. Microbiol. Biotechnol.* **19**, 256–260
7. Jez, J.M., Bennett, M.J., Schlegel, B.P., Lewis, M., and Penning, T.M. (1997) Comparative anatomy of the aldo-keto reductase superfamily. *Biochem J.* **326**, 625–636
8. Mayr, P. and Nidetzky, B. (2002) Catalytic reaction profile for NADH-dependent reduction of aromatic aldehydes by xylose reductase from *Candida tenuis*. *Biochem J.* **366**, 889–899
9. Srivastava, S., Watowich, S.J., Petrash, J.M., Srivastava, S.K., and Bhatnagar, A. (1999) Structural and kinetic determinants of aldehyde reduction by aldose reductase. *Biochemistry.* **38**, 42–54
10. Vander Jagt, D.L., Kolb, N.S., Vander Jagt, T.J., Chino, J., Martinez, F.J., Hunsaker, L.A., and Royer, R.E. (1995) Substrate specificity of human aldose reductase: identification of 4-hydroxynonenal as an endogenous substrate. *Biochim. Biophys Acta.* **1249**, 117–126
11. Davis, R.A. and DeRuiter, J. (1992) Comparison of the catalytic and inhibitory properties of *Pachysolen tannophilus* xylose reductase to rat lens aldose reductase. *Appl. Microbiol. Biotechnol.* **37**, 109–113
12. Kise, S., Koizumi, N., and Maeda, H. (1988) Properties of NAD(P)H-linked aldose-reductase from *Cryptococcus lactativorus*. *J. Ferment. Technol.* **66**, 615–623
13. Neuhauser, W., Haltrich, D., Kulbe, K.D., and Nidetzky, B. (1998) Noncovalent enzyme-substrate interactions in the catalytic mechanism of yeast aldose reductase. *Biochemistry* **37**, 1116–1123
14. Grimshaw, C.E., Bohren, K.M., Lai, C.J., and Gabbay, K.H. (1995) Human aldose reductase: rate constants for a mechanism including interconversion of ternary complexes by recombinant wild-type enzyme. *Biochemistry* **34**, 14356–14365
15. Petrash, J.M., Murthy, B.S., Young, M., Morris, K., Rikimaru, L., Griest, T.A., and Harter, T. (2001) Functional genomic studies of aldo-keto reductases. *Chem. Biol. Interact.* 130–132, 673–683
16. Ditzelmüller, G., Kubicek, C.P., Wöhrer, W., and Röhr, M. (1984) Xylose metabolism in *Pachysolen tannophilus*: Purification and properties of xylose-reductase. *Can. J. Microbiol.* **30**, 1330–1336
17. Rawat, U.B. and Rao, M.B. (1996) Purification, kinetic characterization and involvement of tryptophan residue at the NADPH binding site of xylose reductase from *Neurospora crassa*. *Biochim Biophys Acta.* **1293**, 222–230
18. Verduyn, C., van Kleef, R., Frank, J., Schreuder, H., van Dijken, J.P., and Scheffers, W.A. (1985) Properties of the NAD(P)H-dependent xylose-reductase from the xylose-fermenting yeast *Pichia stipitis*. *Biochem. J.* **226**, 669–677
19. Yokoyama, S.-I., Suzuki, T., Kawai, K., Horitsu, H., and Takamizawa, K. (1995) Purification, characterization and structure analysis of NADPH-dependent D-xylose reductases from *Candida tropicalis*. *J. Ferment. Bioeng.* **79**, 217–223
20. Kavanagh, K.L., Klimacek, M., Nidetzky, B., and Wilson, D.K. (2002), The structure of apo and holo forms of xylose reductase, a dimeric aldo-keto reductase from *Candida tenuis*. *Biochemistry* **41**, 8785–8795
21. Nidetzky, B., Klimacek, M., and Mayr, P. (2001) Transient-state and steady-state kinetic studies of the mechanism of NADH-dependent aldehyde reduction catalyzed by xylose reductase from the yeast *Candida tenuis*. *Biochemistry* **40**, 10371–10381
22. Leitner, C., Neuhauser, W., Volc, J., Kulbe, K.D., Nidetzky, B., and Haltrich, D. (1998) The Cetus process revisited: a novel enzymatic alternative for the production of aldose-free D-fructose. *Biocat. Biotrans.* **16**, 365–382
23. Volc, J., Sedmera, P., Halada, P., Prikrylova, V., and Haltrich, D. (2000) Double oxidation of D-xylose to D-*glycero*-pentos-2, 3-diulose (2, 3-diketo-D-xylose) by pyranose dehydrogenase from the mushroom *Agaricus bisporus*. *Carbohydr Res.* **329**, 219–225
24. Prillinger, H., Messner, R., Koenig, H., Bauer, R., Lopandic, K., Molnar, O., Dangel, P., Weigang, F., Kirisits, T., Nakase, T., and Sigler, L. (1996) Yeasts associated with termites: A phenotypic and genotypic characterization and use of coevolution for dating evolutionary radiations in asco- and basidiomycetes. *System. Appl. Microbiol.* **19**, 265–283
25. Neuhauser, W., Haltrich, D., Kulbe, K.D., and Nidetzky, B. (1997) NAD(P)H-dependent aldose reductase from the xylose-assimilating yeast *Candida tenuis*. Isolation, characterization and biochemical properties of the enzyme. *Biochem. J.* **326**, 683–692
26. Lunzer, R., Mamnun, Y., Haltrich, D., Kulbe, K.D., and Nidetzky, B. (1998) Structural and functional properties of a yeast xylitol dehydrogenase, a Zn^{2+}-containing metalloenzyme similar to medium-chain sorbitol dehydrogenases. *Biochem. J.* **336**, 91–99
27. Ditzelmüller, G., Kubicek-Pranz, E.M., Röhr, M., and Kubicek, C.P. (1985) NADPH-specific and NADH-specific xylose reduction is catalyzed by two separate enzymes in *Pachysolen tannophilus*. *Appl. Microbiol. Biotechnol.* **22**, 297–299
28. Mayr, P., Brüggler, K., Kulbe, K.D., and Nidetzky, B. (2000) D-Xylose metabolism by *Candida intermedia*: isolation and characterisation of two forms of aldose reductase with different coenzyme specificities. *J. Chromatogr. B Biomed. Sci. Appl.* **737**, 195–202
29. Verduyn, C., Frank Jzn., J., van Dijken, J.P., and Scheffers, A.W. (1985) Multiple forms of xylose-reductase in *Pachysolen tannophilus* CBS4044. *FEMS Microbiol. Lett.* **30**, 313–317
30. Askonas, L.J., Ricigliano, J.W., and Penning, T.M. (1991) The kinetic mechanism catalysed by homogeneous rat liver 3 α-hydroxysteroid dehydrogenase. Evidence for binary and ternary dead-end complexes containing non-steroidal anti-inflammatory drugs, *Biochem. J.* **278**, 835–841
31. Penning, T.M. (1999) Molecular determinants of steroid recognition and catalysis in aldo-keto reductases. Lessons from 3α-hydroxysteroid dehydrogenase. *J. Steroid Biochem. Mol. Biol.* **69**, 211–225
32. Hansch, C. and Leo, A. (1995) Exploring QSAR. ACS Professional Reference Book, ACS Washington D.C., USA
33. Angyal, S.J. (1991) The composition of reducing sugars in solution: Current aspects. *Adv. Carbohydr. Chem. Biochem.* **49**, 19–35
34. Grimshaw, C.E. (1992) Aldose reductase: model for a new paradigm of enzymic perfection in detoxification catalysts. *Biochemistry* **31**, 10139–10145
35. Vuorinen, T. and Serianni, A.S. (1990) ^{13}C-substituted pentos-2-uloses: synthesis and analysis by ^{1}H- and ^{13}C-n.m.r. spectroscopy. *Carbohydr. Res.* **207**, 185–210
36. Vander Jagt, D.L., Hassebrook, R.K., Hunsaker, L.A., Brown, W.M., and Royer, R.E. (2001) Metabolism of the 2-oxoaldehyde methylglyoxal by aldose reductase and by glyoxalase-I: roles for glutathione in both enzymes and implications for diabetic complications. *Chem.-Biol. Interact.* 130–132, 549–562

37. Vander Jagt, D.L., Robinson, B., Taylor, K.K., and Hunsaker, L.A. (1992) Reduction of trioses by NADPH-dependent aldo-keto reductases. *J. Biol. Chem.* **267**, 4364–4369
38. Cheng, R.Z., Uchida, K., and Kawakishi, S. (1992) Selective oxidation of histidine residues in proteins or peptides through the copper(II)-catalysed autoxidation of glucosone. *Biochem. J.* **285**, 667–671
39. Uchida, K., Kanematsu, M., Morimitsu, Y., Osawa, T., Noguchi, N., and Niki, E. (1998) Acrolein is a product of lipid peroxidation reaction. Formation of free acrolein and its conjugate with lysine residues in oxidized low density lipoproteins. *J. Biol. Chem.* **273**, 16058–16066